Synthesis, Crystal Structure, and Luminescence Properties of a Novel Green-Yellow Emitting Phosphor $LiZn_{1-x}PO_4:Mn_x$ for Light Emitting Diodes

Ting-Shan Chan,[†] Ru-Shi Liu,*[,†] and Ivan Baginskiy[‡]

Department of Chemistry, National Taiwan University, Taipei 106, Taiwan, and Optical Sciences Center, National Central University, Taoyuan 320, Taiwan

Received October 11, 2007
Revised Manuscript Received December 5, 2007

Since early in 1962, phosphates with the general formula $ABPO_4$ (where A is a monovalent cation and B is a divalent cation) have been of interest for their optical[1] or ferroelectric properties.[2] It is well-known that these phases crystallize into three types of basic structures[3,4] depending on the sizes of the cations, for example, (1) the Na_2SO_4 family, where both A and B are large enough to occupy eight- or nine-coordinated sites; (2) the stuffed tridymite materials, where B is sufficiently small enough to occupy a tetrahedral site; and (3) the olivine-related compounds, where both A and B are located in octahedral sites. The variety in these structures of the $ABPO_4$ family makes it possible to fine-tune a specific physical property or to design a new useful material. It is further advantageous because of the nonlinear optical properties possessed by many of these materials. This makes them attractive for the study of several important technological applications, such as second harmonic generation (SHG), optical switching, and wave guides for optical transmission. The structural and the physical properties of over 200 SHG compounds with general formula $ALiPO_4$ (A = Sr, Ba, Pb) have been studied.[5]

On the other hand, white light emitting diodes (LEDs) can offer benefits in terms of a high luminous efficiency, energy savings, long lifetime, low power consumption, and environmental protection.[6–9] Therefore, LEDs are considered as next generation solid-state light devices. The current research is focused on the development of novel host and phosphor materials with improved luminescence properties for white LEDs, for example, the yellow oxynitride phosphor of Ca-α-SiAlON:$Eu^{2+}$and blue phosphate phosphor of $LiSrPO_4$:Eu^{2+}, respectivity.[10,11] Hence there is an increased interest in the synthsis of new efficient luminescent materials having structures derived from the $ABPO_4$ family. Recently, Eu^{2+}-activated $KSrPO_4$ phosphors emitting strong blue light under UV-light irradiation with excellent thermal stabilities have been reported.[12] However, to the best of our knowledge, there are very few reports on Mn^{2+} doped $LiZnPO_4$ materials for potential applications as a phosphor in LEDs. Therefore the present investigation aims at the synthesis of green-yellow emitting phosphor excitable by a broad UV to blue region as well as study of their crystal structure and luminescence properties.

$LiZn_{1-x}PO_4:Mn_x$ ($0 < x \leq 0.22$) phosphors were synthesized by solid-state reaction. Stoichiometric mixtures of highly pure raw Li_3PO_4, $NH_4H_2PO_4$, ZnO and $MnCO_3$ materials were thoroughly ground and then sintered in argon gas at 900 °C for 4 h followed by sintering at 850 °C for 2 h in a 25% H_2/75% N_2 gas mixture to reduce manganese. The phase purity of the synthesized samples was identified by X-ray diffraction (XRD) analysis using an X'Pert PRO advanced automatic diffractometer with Cu Kα radiation operated at 45 kV and 40 mA. The GSAS program[13] was used for the structure refinements. The UV photoluminescence (PL) and photoluminescence excitation (PLE) spectra were collected at room temperature (RT) using a FluoroMax-3 and FluoroMax-P in the range of 300–500 nm and 470–650 nm, respectively. The quantum efficiency (QE) was also analyzed using PL quantum efficiency measurement system (F-3018 intergrating sphere, HORIBA Jobin Yvon) by a 150 W Xe lamp.

Figure 1a,b shows experimental, calculated, and difference results in the XRD patterns of $LiZn_{1-x}PO_4:Mn_x$ ($x = 0.04$ and 0.12) at RT with $\lambda = 1.5406$ Å. All the observed peaks can be fitted with the reflection conditions in the monoclinic unit cell (space group: *Cc*). The final structural parameters are summarized in Supporting Information, Table S1. Both the atom coordinates and equivalent isotropic temperature factors (Å $\times 10^2$) of $LiZn_{1-x}PO_4:Mn_x$ ($x = 0.12$) are given in Supporting Information, Table S2. The selection bond distances are listed in Supporting Information, Table S3. As seen from Supporting Information, Table S1, Rietveld analysis afforded sufficiently low R (goodness of fit) factors. An increase in lattice parameters and cell volume from $x = 0$ to $x = 0.12$ was observed, which is due to substitution of bigger size Mn^{2+} ions [0.66 Å for CN (coordination number) = 4] as compared to the smaller Zn^{2+} ions (0.60 Å for CN = 4).[14] Moreover, as seen from Supporting Information, Table S3, the Zn−O and P−O bond lengths vary from

* Corresponding author. E-mail: rsliu@ntu.edu.tw.
[†] National Taiwan University.
[‡] National Central University.

(1) Wanmaker, W. L.; Spier, H. L. *J. Electrochem. Soc.* **1962**, *109*, 109.
(2) Blum, D.; Penzin, J. C.; Henrym, J. Y. *Ferroelectric* **1984**, *61*, 265.
(3) Engel, G. *Neues Jahrb. Mineral. Abh.* **1976**, *127*, 197.
(4) Philip, L.; Marian, C. P.; Peter, G. B.; Isaac, A. J. *Mater. Chem* **1991**, *1*, 1061.
(5) Cheryl, S. L.; Hellmut, E.; Thurman, E. C.; Galen, D. S. *Chem. Mater.* **1993**, *5*, 597.
(6) Craford, M. G.; Holonyak, N.; Kish, F. A. *Sci. Am.* **2001**, 815.
(7) Neeraj, S.; Kijima, N.; Cheetham, A. K. *Chem. Phys. Lett.* **2004**, *387*, 2.
(8) Nishida, T.; Ban, T.; Kobayashi, N. *Appl. Phys. Lett.* **2003**, *82*, 3817.
(9) Kim, J. S.; Jeon, P. E.; Choi, J. C.; Park, H. L.; Mho, S. I.; Kim, G. C. *Appl. Phys. Lett.* **2004**, *84*, 2931.
(10) Xie, R. J.; Hirosaki, N.; Sakuma, K.; Yamamoto, Y.; Mitomo, M. *Appl. Phys. Lett.* **2004**, *84*, 5404.
(11) Wu, Z. C.; Shi, J. X.; Wang, J.; Gong, M. L.; Su, Q. *J. Solid State Chem.* **2006**, *179*, 2356.
(12) Tang, Y. S.; Hu, S. F.; Lin, C. C.; Bagkar, Nitin C.; Liu, R. S. *Appl. Phys. Lett.* **2007**, *90*, 151108.
(13) Larson, A. C.; Von Dreele, R. B.; *Generalized Structure Analysis System (GSAS)*; Los Alamos National Laboratory Report LAUR 86-748; Los Alamos National Laboratory: Los Alamos, NM, 1994.
(14) Shannon, R. D. *Acta Crystallogr., Sect. A* **1976**, *32*, 75.

10.1021/cm7028867 CCC: $40.75
Published on Web 01/04/2008

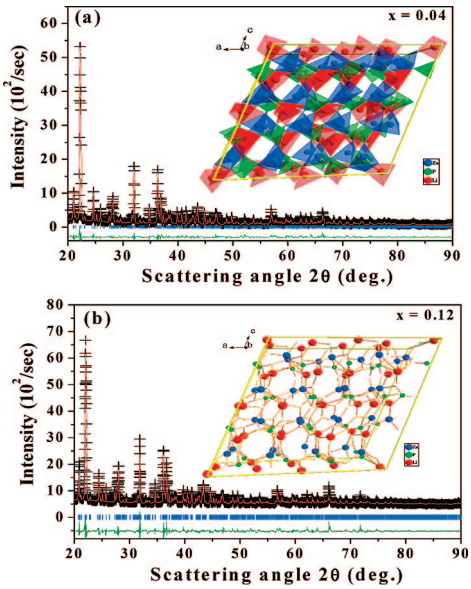

Figure 1. Observed (crosses), calculated (solid line), and difference (bottom) results of XRD profiles of $LiZn_{1-x}PO_4:Mn_x$ for (a) $x = 0.04$ and (b) $x = 0.12$ at RT. Bragg reflections are indicated by tick marks. The ideal structure with $x = 0.04$ viewed along [010]. Green, blue, and red tetrahedrals correspond to PO_4, ZnO_4, and LiO_4, respectively. A stereoplot structure viewed along [010] with $x = 0.12$. The empty circles represent O atoms.

1.921(6) Å for $x = 0.04$ to 1.993(6) Å fro $x = 0.12$ and from 1.516(4) Å for $x = 0.04$ to 1.570(5) Å for $x = 0.12$, respectively. The Li−O bond lengths vary in the range of 1.891(3)−2.025(6) Å. Recently, Xianhui et al.[15] have reported three different structures of $LiZnPO_4$ (LiZn PO_4−CR1, δ-$LiZnPO_4$, and α-$LiZnPO_4$). These structures depend on the proportion and size of the tetrahedra as well as on the temperature. In our case, both the lattice parameters and the β value are similar to those in early reports by Elammari and Elouadi,[16] which indicated that Mn^{2+}-doped $LiZnPO_4$ phosphors have an α-$LiZnPO_4$ type structure. The ideal structure of $LiZn_{1-x}PO_4:Mn_x$ ($x = 0.04$) viewed along [010] is shown in Figure 1a. The structure consists of relatively discrete PO_4 tetrahedra (green color) linked by distorted ZnO_4 (blue color) and LiO_4 (red color) tetrahedra. A stereoplot of the $LiZn_{1-x}PO_4:Mn_x$ ($x = 0.12$) structure viewed along [010] is given in Figure 1b. The empty circles represent O atoms which are shared by three tetrahedra in the α-$LiZnPO_4$ structure.

The excitation (PLE) and emission (PL) spectra of a selected $LiZn_{1-x}PO_4:Mn_x$($x = 0.1$) sample is shown in Figure 2. The PLE spectrum (300–550 nm) shows five lines centered at 350, 375, 414, 431, and 464 nm corresponding to the well-known transitions of Mn^{2+} ion from ground level $^6A_1(^6S)$ to $^4E(^4D)$, $^4T_2(^4D)$, $[^4A_1(^4G), ^4E(^4G)]$, $^4T_2(^4G)$, and $^4T_1(^4G)$ excited levels, respectively.[17] Moreover, the PL spectrum (450–650 nm) consists of one broad symmetric line attributed to the spin-forbidden $d-d$ transition ($^4T_1$ (^4G) → $^6A_1(^6S)$) of Mn^{2+} and centered in the wavelength range of 550–560 nm depending on the Mn content in $LiZn_{1-x}PO_4:Mn_x$. Both

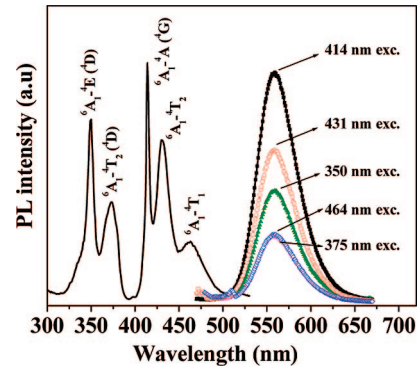

Figure 2. UV PL and PLE spectra of $LiZn_{1-x}PO_4:Mn_x$ ($x = 0.1$).

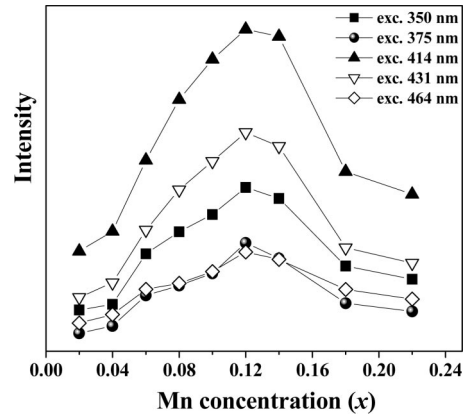

Figure 3. Emission intensity vs manganese concentration (x) of $LiZn_{1-x}PO_4:Mn_x$ phosphor under various excitation wavelengths.

the peak position and the shape of the emission spectrum are independent of excitation wavelength; this indicates there is only one emission center in the phosphor and confirms that the activator ions (Mn^{2+}) occupy only equivalent positions in the $LiZnPO_4$ host lattice.

The dependences of PL intensities of $LiZn_{1-x}PO_4:Mn_x$ phosphors with various concentrations of Mn ($x = 0.02$, 0.04, 0.06, 0.08, 0.1, 0.12, 0.14, 0.18, 0.22) excited by different excitation wavelengths are shown in Figure 3. The PL intensity for all excitation wavelengths increased with increasing Mn concentration until a maximum intensity is reached at $x = 0.12$, and then it decreased as a result of concentration quenching.[12,18] The fluorescence mechanism of Mn^{2+} in $LiZn_{1-x}PO_4:Mn_x$ phosphors can be proposed as follows.

The emission intensity (I) per activator ion is given by the equation[19–21]

$$I/x = K[1 + \beta(x)^{Q/3}]^{-1} \quad (1)$$

were x is the activator concentration; $Q = 6$, 8, or 10 is for dipole–dipole, dipole–quadrupole, or quadrupole−quadrupole interaction, respectively; and K and β are constants for the same excitation condition for a given host crystal.

It can be seen from Figure 4 that the plot of $\log(x\mathrm{Mn}^{2+})$ vs $\log[I/x\mathrm{Mn}^{2+}]$ in the selected $LiZn_{1-x}PO_4:Mn_x$ ($\lambda_{ex} = 414$ nm) sample is linear and the slope is −0.84. By using the

(15) Xianhui, B.; Thurman, E. G.; Galen, D. S. *J. Solid State Chem.* **1998**, *138*, 126.
(16) Elammari, L.; Elouadi, B. *Acta Crystallogr., Sect. C* **1989**, *45*, 1864.
(17) Su, F.; Ma, B.; Ding, K.; Li, G.; Wang, S.; Chen, W.; Joly, A. G.; McCready, D. E. *J. Lumin.* **2006**, *116*, 117.
(18) Lucas, F.; Jaulmes, S.; Quarton, M. *J. Solid State Chem.* **2000**, *150*, 404.
(19) Van Uitert, L. G. *J. Electrochem. Soc.* **1967**, *114*, 1048.
(20) Ozawa, L.; Jaffe, P. M. *J. Electrochem. Soc.* **1971**, *118*, 1678.
(21) Wang, Q. Z.; Tian, J.; Yang, X. H.; Gao, X. *J. Chin. Lumin.* **1995**, *16*, 57.

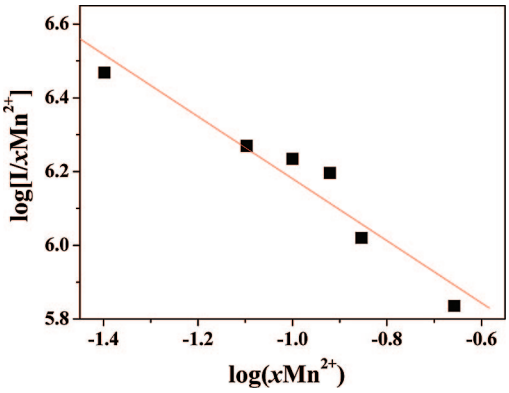

Figure 4. Plot of $\log(x\mathrm{Mn}^{2+})$ vs $\log[\mathrm{I}/x\mathrm{Mn}^{2+}]$ in $\mathrm{LiZn}_{1-x}\mathrm{PO}_4{:}\mathrm{Mn}_x$ phosphor ($\lambda_{ex} = 414$ nm).

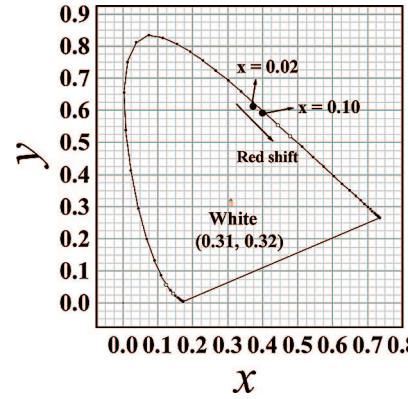

Figure 5. CIE chromaticity diagram of $\mathrm{LiZn}_{1-x}\mathrm{PO}_4{:}\mathrm{Mn}_x$ ($x = 0.02$ and 0.10).

above eq 1, the Q value obtained is 5.52, which is approximately equal to 6. The result indicates that the dipole–dipole interaction is the major mechanism for concentration quenching of the central Mn^{2+} emission in $\mathrm{LiZn}_{1-x}\mathrm{PO}_4{:}\mathrm{Mn}_x$ phosphors. In addition, as seen from Supporting Information, Figure S1, by comparing the commercial yellow standard phosphor (e.g., YAG:Ce), the emission intensity of $\mathrm{LiZn}_{1-x}\mathrm{PO}_4{:}\mathrm{Mn}_x$ ($x = 0.12$) under 414 nm excitation is about 34% for YAG:Ce under 460 nm excitation. Moreover, the obtained internal QEs of YAG:Ce and $\mathrm{LiZn}_{1-x}\mathrm{PO}_4{:}\mathrm{Mn}_x$ ($x = 0.12$) are about 92% and 81%, respectively.

To observe the effect of the doping of Mn^{2+} on CIE chromaticity of the phosphate based phosphor, we prepared a series of $\mathrm{LiZn}_{1-x}\mathrm{PO}_4{:}\mathrm{Mn}_x$ phosphors ($x = 0.02$ and 0.1). Figure 5 shows the chromaticity points of $\mathrm{LiZn}_{1-x}\mathrm{PO}_4{:}\mathrm{Mn}_x$. As the concentration of Mn is increased, the CIE coordinates (x, y) were varied systematically from $x = 0.02$ of (0.388, 0.601) to $x = 0.1$ of (0.399, 0.592). They are located between green and yellow regions. Change in positions from $x = 0.02$ to $x = 0.1$ confirms a noticeable shift of emission to a longer wavelength (red shift) region with increasing content of the activator. The phenomena can be explained by exchange interactions between Mn^{2+} ions pairs or some change in the crystal field surrounding the activator cations.[10,22]

In summary, we have synthesized successfully a novel green-yellow emitting phosphor $\mathrm{LiZn}_{1-x}\mathrm{PO}_4{:}\mathrm{Mn}_x$ and investigated its structural and luminescence properties. Moreover, we have shown that these materials can be tuned from green to yellow under ultraviolet radiation by varying Mn^{2+} dopant in the host matrix. Thus $\mathrm{LiZn}_{1-x}\mathrm{PO}_4{:}\mathrm{Mn}_x$ can be potentially useful as a UV radiation-converting phosphor for LEDs.

Acknowledgment. The authors would like to express their appreciation for financial support from the National Science Council (Contract No. NSC 96-2120-M-002-019), the Ministry for Economic Affairs (Contract No. 96-EC-17-A-07-S1-043), Taiwan, and the Epistar Corporation (Hsinchu, Taiwan).

Supporting Information Available: Details of the structure refinement of $\mathrm{LiZn}_{1-x}\mathrm{PO}_4{:}\mathrm{Mn}_x$ ($x = 0.04$ and 0.12) [Tables S1–S3] and UV PL and PLE spectra of $\mathrm{LiZn}_{1-x}\mathrm{PO}_4{:}\mathrm{Mn}_x$ ($x = 0.12$) and commercial yellow standard phosphor YAG:Ce (Figure S1) (PDF). This material is available free of charge via the Internet at http:/pubs.acs.org.

CM7028867

(22) Ronda, C. R.; Amrein, T. *J. Lumin.* **1996**, *69*, 245.